2. SITE 395[1]

Shipboard Scientific Party[2]

HOLE 395A

Position: 22°45.3519′N, 46°4.8609′W

Start hole: 0700 hr, 28 July 1997

End hole: 0230 hr, 1 August 1997

Time on hole: 91.5 hr (3.81 days)

Seafloor (drill-pipe measurement from rig floor, mbrf): 4494

Total depth (drill-pipe measurement from rig floor, mbrf): not checked

Distance between rig floor and sea level (m): 11.5

Water depth (drill-pipe measurement from sea level, m): 4482.5

Comments: Reenter, log, and CORK operation in existing hole.

Principal results: The main objective of Leg 174B was to reenter Hole 395A for a selected suite of downhole logs followed by installation of an instrumented borehole seal or Circulation Obviation Retrofit Kit (CORK). The purposes of the logs and CORK experiment were (1) to document the in situ physical properties and hydrogeology at this young crustal reference site, and (2) to test a hydrological model developed from observations obtained during three earlier reentries since the hole was drilled over 21 yr ago in 1975−1976. Leg 174B operations at Hole 395A were very successful in achieving these objectives.

Leg 174B represents the fourth time Hole 395A has been reentered since it was drilled on Ocean Drilling Program (ODP) Leg 45 (1975–1976). It was reentered for logging and downhole experiments during Legs 78B (1981) and 109 (1986), and using the French submersible *Nautile* during the Dianaut reentry expedition (1989). Past observations from Hole 395A indicate a continuous downhole flow of ocean bottom water and generally support a model of lateral flow of seawater in the upper basement beneath the sediment pond in which the site is located. The logs and CORK experiment deployed during Leg 174B will provide essential information about the formation pressure and permeability structure, which are keys to understanding the crustal hydrogeology at the site.

Initial shipboard interpretation of the Davis-Villinger Temperature Probe (DVTP) and Schlumberger logs supports the following preliminary results. Like all past temperature logs in Hole 395A, the DVTP and temperature-logging tool (TLT) logs show virtually isothermal borehole temperatures from seafloor down to 350 mbsf. From 350 to 450 mbsf there is a slight increase in temperature; below 450 mbsf there is a much stronger increase in temperature. This reconfirms prior indications of a strong flow of ocean bottom water down the hole, at a rate of 1000–2000 L/hr, exiting into the formation between casing and 450 mbsf. Shipboard analyses of the Leg 174B Schlumberger logs and comparisons to Leg 45 core descriptions and logs from Legs 78B and 109 clearly show that Hole 395A consists of definable layers of pillow basalts, massive flows, and fluid aquifers that correlate to changes in the resistivity, velocity, and bulk density logs. Distinct changes in the high-resolution temperature gradient log and anomalies in the spontaneous potential (SP) log indicate that at least two major aquifers are active in the hole at approximately 310 and 420 mbsf. Zones of high resistivity and high sonic velocity distinguish massive lava flows, and both resistivity and velocity generally increase towards the bottom of the hole. High-resolution borehole images, cement bond quality, formation strength, and elastic properties can be extracted from the FMS and DSI logs. The ARI data produced images that show the character and orientation of individual pillow basalts and the heterogeneity of crustal structures at a vertical scale of ~1 m. From the comparison of FMS and ARI images, the extent of pillows and flows near the borehole may also be distinguished.

CORK data were successfully recovered in late January of 1998 (Becker and Davis, 1998; Becker et al., 1998), utilizing *Nautile*, but are not included in this report. The features of the log data described above are particularly relevant to the hydrogeologic structure in Hole 395A and illustrate the physical state of the ocean crust in unprecedented detail. Overall, the Leg 174B logging program has solidified the position of Hole 395A as the most important reference hole for young oceanic crust formed at a slow spreading rate.

BACKGROUND AND OBJECTIVES

The main objective of Leg 174B was to reenter Hole 395A (Fig. 1) for a selected suite of downhole logs followed by installation of an instrumented borehole seal or Circulation Obviation Retrofit Kit (CORK; Davis et al., 1992). The purposes of the logs and CORK experiment were (1) to document the in situ physical properties and hydrogeology at this young crustal reference site, and (2) to test a hydrological model developed from observations obtained during three earlier reentries since the hole was drilled over 21 yr ago in 1975–1976. The observations from Hole 395A generally support a model of lateral flow of seawater in the upper basement beneath the sediment pond in which the site is located. The logs and CORK experiment provide essential information about the formation pressure and permeability structure, which are keys to understanding the crustal hydrogeology at the site.

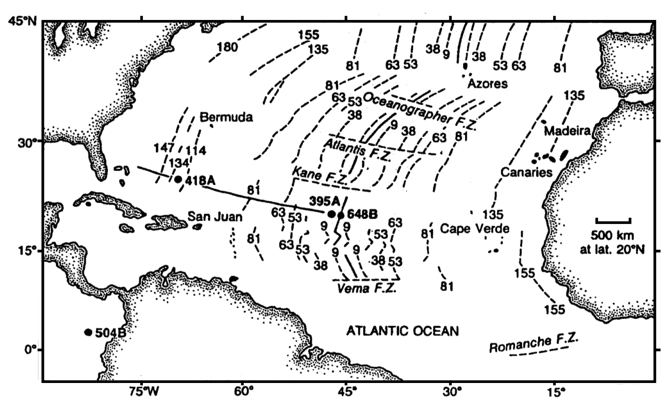

Figure 1. Locations of Holes 395A, 418A, 504B, and 648B. Dashed lines show ages of crust in Ma, deduced from magnetic anomalies (after Hyndman, Salisbury, et al., 1984).

[1]Becker, K., Malone, M.J., et al., 1998. *Proc. ODP, Init. Repts.,* 174B: College Station, TX (Ocean Drilling Program).
[2]Shipboard Scientific Party is given in the list preceding the Table of Contents.

Background

Only a handful of Deep Sea Drilling Project (DSDP)/Ocean Drilling Program (ODP) holes penetrate more than 500 m into “normal” oceanic crust formed at mid-ocean ridges, and these are all, therefore, important reference holes. Among them, Holes 395A and 504B (Fig. 1) form the most important pair of reference sites for young, upper oceanic crust formed at slow and medium spreading rates, respectively. They are particularly important as reference sites for the hydrogeology of young oceanic crust, which has been studied with extensive downhole measurements and detailed heat-flow surveys at both sites (e.g., Fig. 2). Holes 395A and 504B are the best documented of several cases in which ocean bottom water is known to be flowing down open DSDP/ODP holes into permeable levels of upper basement. These examples suggest that young upper oceanic crust under a sediment cover is easily permeable enough to support active circulation of seawater, but we still barely understand the details of such off-axis hydrothermal circulation or its control by the pressure distribution and fine-scale permeability structure.

Site 395 is located in 7-Ma crust, in an isolated sediment pond with low heat flow (Hussong et al., 1979; Langseth et al., 1992) that might be considered somewhat typical of the structure and hydrogeological setting for thinly sedimented crust formed at slow spreading rates. Since it was drilled in 1975–1976 (Shipboard Scientific Party, 1979), Hole 395A has been revisited three times for an extensive set of downhole measurements: during DSDP Leg 78B in 1981 (Hyndman, Salisbury, et al., 1984), during ODP Leg 109 in 1986 (Bryan, Juteau, et al., 1988), and during the French wireline reentry campaign DIANAUT in 1989 (Gable et al., 1992). The hole was originally drilled during Leg 45 to a depth of 664 m, or 571 m into basement, but bad hole conditions were encountered in the deepest 50 m (Shipboard Scientific Party, 1979). When the hole was revisited five years later during Leg 78B, the deepest 55 m of the hole were blocked by fill (Hyndman, Salisbury, et al., 1984). However, very similar total hole depths were registered during Leg 109 and the DIANAUT program, indicating that hole conditions apparently stabilized shortly after Leg 45, with a total open-hole length of ~606 m, 513 m into basement.

On each of three prior reentries of Hole 395A, the first order of business was temperature logging in the hole long after it had reequilibrated from any prior disturbance by DSDP/ODP operations. Each of the three temperature logs showed strongly depressed borehole temperatures, essentially isothermal to a depth of ~300 m into basement (Becker et al., 1984; Kopietz et al., 1990; Gable et al., 1992). Packer and flowmeter experiments conducted during prior reentries indicate that this section of basement is much more permeable than the underlying formation (Hickman et al., 1984; Becker, 1990; Morin et al., 1992). The near-isothermal temperatures in the upper part of the hole indicate a strong downhole flow of ocean bottom water into permeable upper basement, at rates of thousands of liters per hour, virtually unabated over the 21 yr that the hole has been open (Fig. 3). In that time, it is estimated that a total of over 200,000,000 L of ocean bottom water has been drawn down the hole into the subseafloor hydrogeologic system at Site 395.

In comparison, temperatures measured during the multiple revisits to Hole 504B were initially strongly depressed to a depth of ~100 m into basement, but then rebounded nonmonotonically towards a conductive profile. This indicates that the rate of downhole flow in that hole has decayed since the hole was first drilled, and that the downhole flow is directed into a more restricted section of uppermost basement than in Hole 395A (Becker et al., 1983a, 1983b, 1985, 1989; Gable et al., 1989; Guerin et al., 1996). The comparison suggests that Hole 504B penetrates a more passive hydrothermal regime, whereas Hole 395A provides a man-made shunt into a more active circulation system in basement. The various observations at Site 395 generally support a model proposed by Langseth et al. (1984, 1992; Fig. 4) for lateral circulation in the upper basement beneath the sediment pond where the hole is sited, but we have little resolution on any details of such circulation.

A number of holes drilled into young oceanic crust have proven to be drawing ocean bottom water down into permeable levels of basement (e.g., Erickson et al., 1975; Hyndman et al., 1976; Ander-

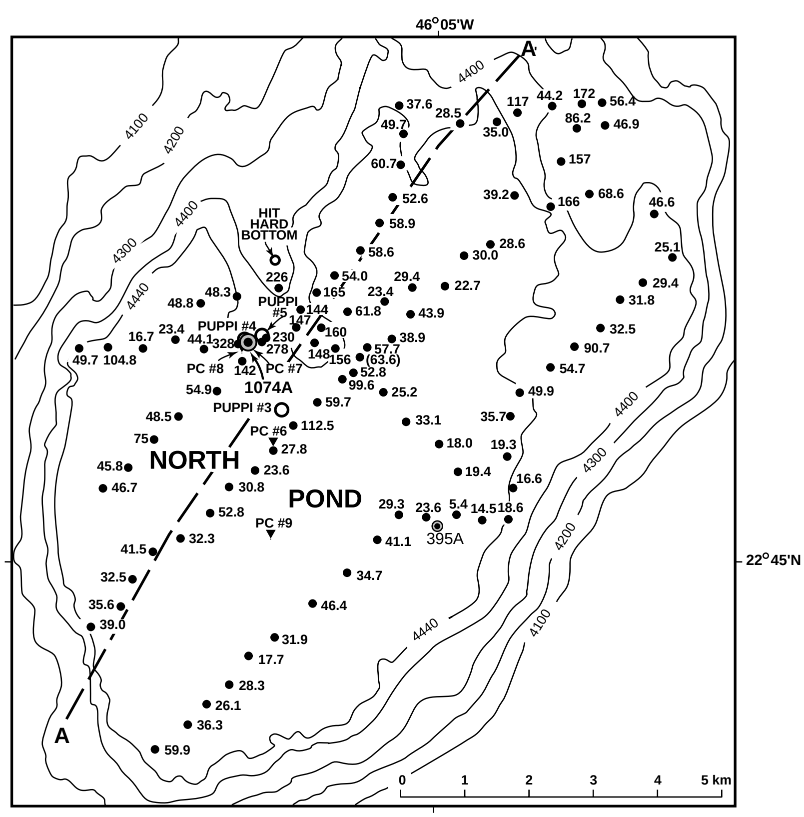

Figure 2. Locations of heat-flow measurements, pop-up pore pressure instrument (PUPPI) deployments, piston cores, and Hole 395A in North Pond. Heat-flow values are given in mW/m^2 (from Langseth et al., 1992).

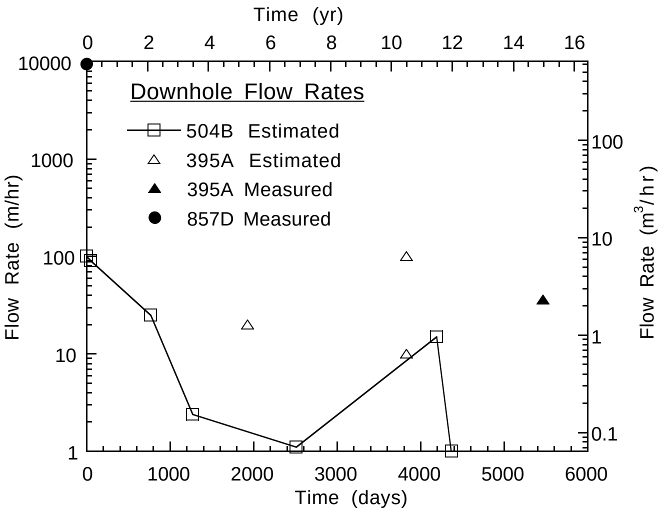

Figure 3. Measured and estimated downhole flow rates in the three best documented cases, Holes 395A, 504B, and 857D. Data sources for Holes 395A and 504B are given in text; Hole 857D results are from Becker et al. (1994).

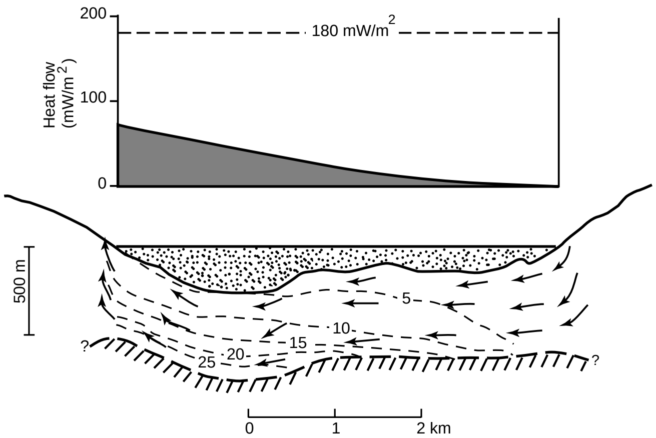

Figure 4. Schematic model of pore-water flow and isotherms (°C) beneath North Pond and surface heat flow, assuming laminar lateral flow rate of ~1 mm/yr (from Langseth et al., 1984).

son and Zoback, 1982; Becker et al., 1983a, 1983b, 1984; Davis, Mottl, Fisher, et al., 1992). Such downhole flow requires sufficient basement permeability and a differential pressure between the fluids in the borehole and the formation fluids. In general, we surmise that the necessary differential pressures may arise because of some combination of two independent effects.

1. The differential pressure (which should not be termed an "underpressure") between the cold, dense seawater used as drilling fluid in the borehole and the warmer formation fluids.
2. True, dynamically maintained underpressures caused by active circulation in the basement that would occur even if the borehole were not present.

In cases of downhole flow in holes drilled into formations with high geothermal gradients, the driving force is probably dominated by the former effect (e.g., ODP Leg 139 sites in Middle Valley; Davis, Mottl, Fischer, et al., 1992). For holes such as Hole 504B, both effects may be important. In holes drilled into young crust with low geothermal gradients, such as Hole 395A, the latter effect may be predominant.

Objectives and Methods

By leaving Hole 395A open for over 20 yr, with revisits for discrete data sampling roughly every 5 yr, we have only learned that the downhole flow has apparently continued at a significant rate. We have no resolution as to possible variations in downhole flow rates with time (as has been documented in Hole 504B), let alone the constancy or variability of the driving forces responsible for the downhole flow. Furthermore, we still do not understand exactly where the downhole flow is directed in the formation, other than the general statement that it is directed into the upper 300 m or so of basement.

The Leg 174B program was designed to address these important issues by providing essential information about the in situ physical properties, permeability structure, and formation pressure, which are keys to understanding the crustal hydrogeology at Site 395. With ~5 days to be spent at Hole 395A during Leg 174B, the operational program was scheduled to begin with ~3 days of logging, followed by ~2 days for installation of a CORK. These were planned in a sequence requiring two trips of the drill string, as follows:

1. Logs: After initial reentry with a logging bottom-hole assembly (BHA), a temperature log with the Davis Villinger Temperature Probe (DVTP), followed by three Schlumberger logs to delineate the fine-scale permeability structure of the open-hole section penetrated by Hole 395A. The three Schlumberger logs included two advanced sondes run for the first time in an ODP hole, the ARI and the DSI (see "Introduction" chapter, this volume). A flowmeter was also prepared for possible use, but was not deployed for several reasons.
2. CORK: Deployment of a fully configured CORK to seal the hole, instrumented with a 595-m-long, 10-thermistor cable, a pressure sensor in the sealed section, and a reference pressure sensor at seafloor depth.

The CORK installation will provide a long-term record (5 yr or longer) of (1) the rebound of temperatures and pressures toward formation conditions after the emplacement of the seal, (2) possible temporal variations in temperatures because of lateral flow in discrete zones, and (3) pressure variations, which in a sealed hole would be the primary manifestation of changes in the forces that drive the natural circulation system. The first installment of data from the CORK experiment was collected during January 1998, utilizing the French submersible *Nautile,* with support from the National Science Foundation (Becker and Davis, 1998; Becker et al., 1998).

The primary purpose of the CORK experiment is not necessarily to assess the equilibrium predrilling thermal regime (which we can estimate from detailed heat-flow surveys as in Fig. 2), but instead to monitor how the hydrologic system varies with time as natural hydrogeological conditions are reestablished. Full thermal reequilibration could require many tens or hundreds of years if it occurs only by conductive processes, but could also occur in much less time if the Langseth et al. (1984, 1992) model of active lateral circulation is correct. We are interested primarily in exploring the causes of the hydrogeological state and any possible temporal variations, with the simplest goal to determine how these are associated with and controlled by formation pressure and/or permeability structure. It is impossible to model or predict all of the possible outcomes of the experiment, but considering two possible end-member results might be instructive.

1. If the model of active lateral circulation is basically incorrect, and downhole flow is indeed simply an artifact of drilling, then sealing the hole should remove the driving force for the downhole flow, and temperatures and pressures will slowly and smoothly trend toward values consistent with conductive, hydrostatic processes.
2. If there is some element of truth to the model of active lateral circulation in basement, with this circulation providing the driving pressure differential for the downhole flow, then seal-

ing the hole will not change the driving force, and lateral circulation should continue even though the seal has stopped the downhole flow. Pressures in the sealed hole should approach a nonhydrostatic value in an irregular fashion that reflects variability in the natural hydrogeologic processes. Similarly, temperatures will rebound towards values consistent with the circulation system, also in an irregular fashion that reflects natural hydrogeologic variability. In addition, differences in the behavior of the temperature sensors should reflect vertical variations in the lateral flow regime because of fine-scale permeability variations. We understand so little about crustal hydrogeology that simply defining the natural time and space scales of such variability will be a very important result.

OPERATIONS

Transit To Hole 395A

The ship departed at 1600 hr (EST) on 21 July, 1997 from New York. The 1768-nmi (3274 km) sea voyage to Hole 395A was completed in 154.5 hr at an average speed of 11.4 kt. All subsequent times reported in this operations section are local time (UTC −2 hr), unless otherwise noted.

Hole 395A

The ship arrived on location at Hole 395A at 0700 hr on 28 July. Following deployment of a beacon, reentry/logging BHA, and reentry video system, the seafloor was tagged at 4494 mbrf or 4482.5 mbsl. The reentry cone was located and reentered in 3 hr, nearly 100 m northeast of the last reported coordinates. The bit was then positioned at 32 mbsf for logging. The DVTP was run first on the coring line, logging temperatures during 5-min station stops every 20 m down the hole. This was followed by three Schlumberger logging runs, including two advanced sondes never before deployed in ODP crustal holes: the ARI and the DSI. The first tool string included the ARI, spectral gamma ray (HNGS), and Lamont high-resolution temperature-logging (TLT) sondes; excellent data were acquired from 603 mbsf to the bottom of casing at 113 mbsf. The second tool string included the spectral gamma ray (NGT), DSI, and FMS tools. Three passes of this string in the open-hole section were run using the DSI in conventional monopole, in-line and cross-dipole, and Stoneley-wave recording modes, respectively. Good to excellent FMS and compressional and shear-waveform data were collected during the first two passes, with the exception of two enlarged intervals near 120 and 420 mbsf. Data from the third pass are of lesser quality, partly because of an electronic fault that precluded further use of the wireline heave compensator. The third triple-combo tool string included the spectral gamma ray (HNGS), the advanced porosity sonde (APS), the lithodensity sonde (LDS), and the DITE. The entire hole was logged up to the seafloor without using the wireline heave compensator, and a repeat log was run from 136 to 106 mbsf. The data are of excellent quality, with the exception of the two hole enlargements near 120 and 420 mbsf, where the density and neutron porosity tools lost contact with the borehole wall. A spontaneous potential (SP) log was also acquired over the open-hole interval. Throughout the logging operations, good hole conditions were encountered down to 603 mbsf, and it was never necessary to run the bit beyond 32 mbsf into open hole for cleanout operations.

After the logging operations, Hole 395A was successfully sealed with a CORK, instrumented with a long-term data logger, pressure gauges above and below the seal, and cable with 10 thermistors (at 98, 173, 248, 298, 348, 398, 448, 498, 548, and 598 mbsf). The data logger was positively latched into the CORK body, but the CORK body could not be mechanically latched into the casing. However, the CORK was seen on video to be in proper position, and the lack of a mechanical latch should not compromise the experiment; the seals are in proper position and the 21-yr history of downhole flow in Hole 395A suggests that there is virtually no possibility that the formation will develop positive pressures large enough to displace the CORK and breach the seals. The CORK running assembly arrived on deck at 0230 hr on 1 August, ending operations in Hole 395A.

CORK/DVTP

DVTP Temperature Log

Upon the initial reentry of Hole 395A, the bit was run into the hole only to 31.7 mbsf, leaving the interval 32−606 mbsf completely undisturbed for a temperature log. The DVTP, normally used for temperature measurements in sediments, was run on the coring line into open hole to obtain the temperature log. The tool was run for 30 station measurements of 5-min duration at 20-m intervals from 4500 to 5080 mbrf, with depths determined by the coring winch. The DVTP was also used to tag bottom, which was expected at 5100 mbrf but was encountered at an apparent depth of 5125 mbrf; after bottom was tagged, the tool was pulled back to 5110 mbrf for a final station measurement. Although the coring winch was carefully zeroed before the log with the DVTP probe at the rig floor, the apparent total depth measured during this run is well beyond the known depth of the hole, 5100 mbrf, as determined during Leg 109 (Shipboard Scientific Party, 1988). In contrast, total hole depth of 5097 mbrf as measured immediately after the DVTP with the Schlumberger logs (see “Downhole Logging” section, this chapter) was in close agreement with the Leg 109 depth. Therefore, depths of the DVTP stations were corrected to depths in meters below seafloor by scaling the coring winch reading by 5097/5125, and then subtracting the seafloor depth as measured by the drill pipe, 4194 mbrf.

Figure 5 shows the temperature-time data from the DVTP run, illustrating the rapid equilibration and stability of probe temperatures at each depth. Figure 6 shows the temperature-depth profile obtained from the log. It is immediately obvious that the profile is very similar to past profiles measured by Becker et al. (1984), Kopietz et al., (1990), and Gable et al. (1992). Like these past profiles, the DVTP log is virtually isothermal down to 300−400 mbsf, indicating downhole flow of ocean bottom water through the casing and into the upper 300 m of basement. The similarity of profiles also argues for a near constancy of the downhole flow rate, previously estimated at ~1000−2000 L/hr (Becker et al., 1984; Morin et al., 1992). The Schlumberger logs (see “Downhole Logging” section, this chapter) conducted after the DVTP run identified several possible zones that probably accept the downhole flux of bottom water. Also notable are

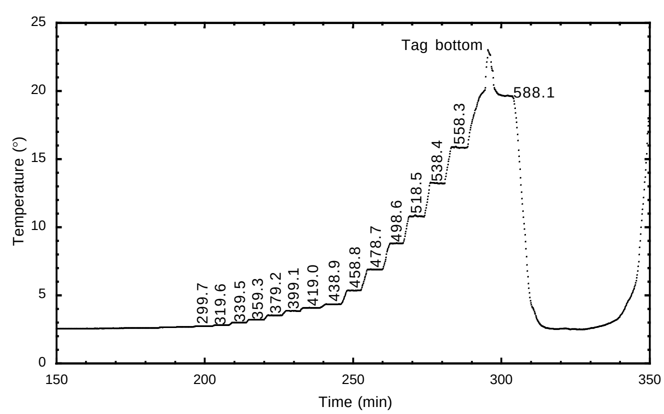

Figure 5. Temperature−time record of the DVTP temperature log in Hole 395A. Below the essentially isothermal upper section, corrected depths of measurement points are noted in meters below seafloor.

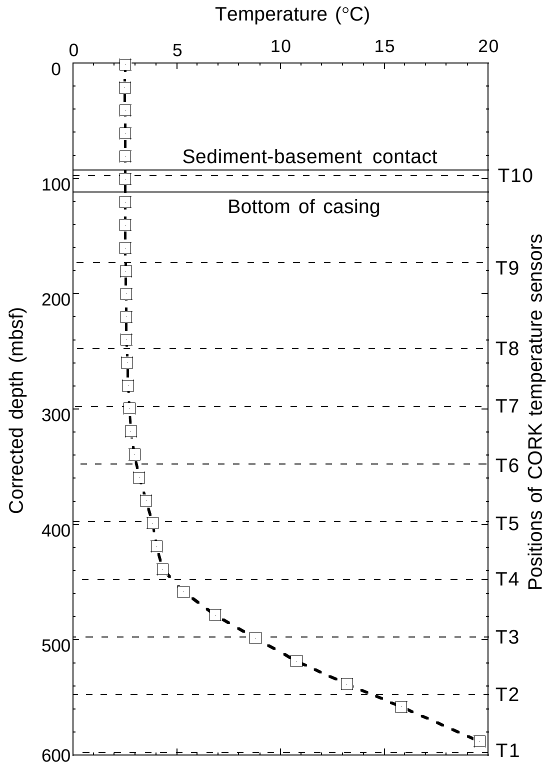

Figure 6. DVTP temperatures vs. corrected depth in Hole 395A. Also shown are the positions of thermistors deployed in the hole in the CORK experiment.

inflection points in the DVTP profile at ~350 and 450 mbsf. The strong inflection at 450 mbsf probably marks the lower limit of the downhole flow, and the less obvious inflection at 350 mbsf probably marks the lower limit of a zone accepting a major portion of the downhole flow.

CORK Experiment

After the Schlumberger logs, a CORK observatory was successfully emplaced in Hole 395A. The purpose of this experiment was to seal the hole, thereby shutting off the long-lived downhole flow of ocean bottom water and allowing long-term monitoring of in situ temperatures and pressures in upper basement. As described by Davis et al. (1992), each CORK consists of a seal in the reentry cone, a long-term data logger, a pressure sensor inside the seal as well as a reference pressure gauge outside the seal, and a cable with 10 thermistors. The positions of the temperature sensors on the cable deployed in Hole 395A are shown with the DVTP temperature log in Figure 6. No data were available from the CORK experiment during Leg 174B; the first data were recovered in late January of 1998 using the French submersible *Nautile* (Becker and Davis, 1998; Becker et al., 1998).

Operations during the deployment of the CORK experiment were smooth except for one important factor: although the data logger was successfully latched into the CORK body, the latch between the CORK body and reentry cone could not be engaged. Thus, while the CORK seals are in proper position, there is no mechanical device holding the CORK in the reentry cone and casing. However, the 21-yr history of downhole flow suggests that fluid pressures in the sealed hole are not likely to exceed hydrostatic; more likely, the formation will remain at or less than hydrostatic pressure, so the lack of a mechanical latch should not compromise the hydraulic seal essential to the CORK experiment.

DOWNHOLE LOGGING

Operations

Hole 395A was reentered and logged before CORK operations using three wireline tool strings. Logging operations began at 0200 hr, 29 July 1997. The first tool string was 22 m long and included the ARI, HNGS, and TLT sondes. This was the debut deployment of the deep-penetrating ARI in an ODP hole. The pipe was set at 32 mbsf and the wireline heave compensator was used. The log was run uphole at 550 m/hr from 603 mbsf to the casing shoe at 113 mbsf. A repeat log was run from 236 to 181 mbsf. Total rig time used for this run was 7.75 hr. The data are of excellent quality and, in general, hole conditions are good. Image processing of the ARI data was accomplished using shipboard software.

The second tool string included the NGS, DSI, and FMS tools, having a total length of 33 m. This was the first use of the DSI tool in the ocean crustal rocks. Three passes of this string were run using the DSI in conventional monopole, in-line and cross-dipole, and Stoneley-wave recording modes. Switching between recording modes was accomplished while the tool was downhole. Pass 1 was run uphole at 275 m/hr from 603 mbsf to the casing shoe at 113 mbsf to record the data-intensive FMS and compressional and shear DSI modes. Pass 2 was run uphole from 603 mbsf in open hole, then through casing to the seafloor, with two dipole recording modes enabled. Excellent FMS and compressional and shear-waveform data were collected during Passes 1 and 2 with the exception of two enlarged intervals near 120 and 420 mbsf, where the FMS pads lost contact with the borehole wall and are unreliable. Pass 3 was run uphole from 603 mbsf to casing, with the low-frequency Stoneley and the cross-dipole recording modes enabled. The Pass 3 FMS logs are of lower quality because of an electronic fault that precluded further use of the wireline heave compensator. The DSI Stoneley mode also produced erratic waveforms that are not reliable. After some difficulty pulling the FMS back into the drill pipe, 14 hr of rig time were used for this run.

The third triple-combo tool string was 31.5 m long and included the HNGS, APS, LDS, and DITE. One run was made uphole at 550 m/hr from 603 mbsf to the seafloor without using the wireline heave compensator. A repeat log was run from 136 to 106 mbsf. The data of are excellent quality, with the exception of the two hole enlargements near 120 and 420 mbsf where the density and neutron porosity tools lose contact with the borehole wall and are unreliable. An SP log was also acquired over the open-hole interval. Total rig time for this run was 7 hr. Logging operations were completed at 0645 hr, 30 July 1997, using a total of 28.75 hr of rig time.

Borehole Condition and Log Data Quality

Shipboard analysis of the logs and core descriptions during Leg 45, Leg 78B, Leg 109, and Leg 174B clearly shows that Hole 395A consists of definable layers of pillow basalts, massive flows, and fluid aquifers that correlate to changes in the measured log properties. The state-of-the-art logs run during Leg 174B provided extraordinarily high-quality results and can be used to significantly enhance our understanding of the hydrogeology of the upper ocean crust.

A selection of most of the logs acquired in three runs during Leg 174B are presented in Figures 7 and 8. The interval displayed corresponds to the total depth of Hole 395A, from 603 mbsf to the seafloor; the data were acquired in open hole from total depth (TD) to the base of casing at 113 mbsf, all in crustal rocks. The nuclear and sonic logs were also run through the casing to the seafloor, and repeat passes were made for quality control, but are not shown. Two caliper logs from the FMS tool are shown in Figure 7 (Track 1) and illustrate two orthogonal dimensions of the borehole as a function of depth. The diameter of Hole 395A varies generally between 10 and 16 in, with two severe washouts at ~163–176 mbsf and 418–430 mbsf with rapid variations between 12 and 15 in from 210 to 240 mbsf. Otherwise, the

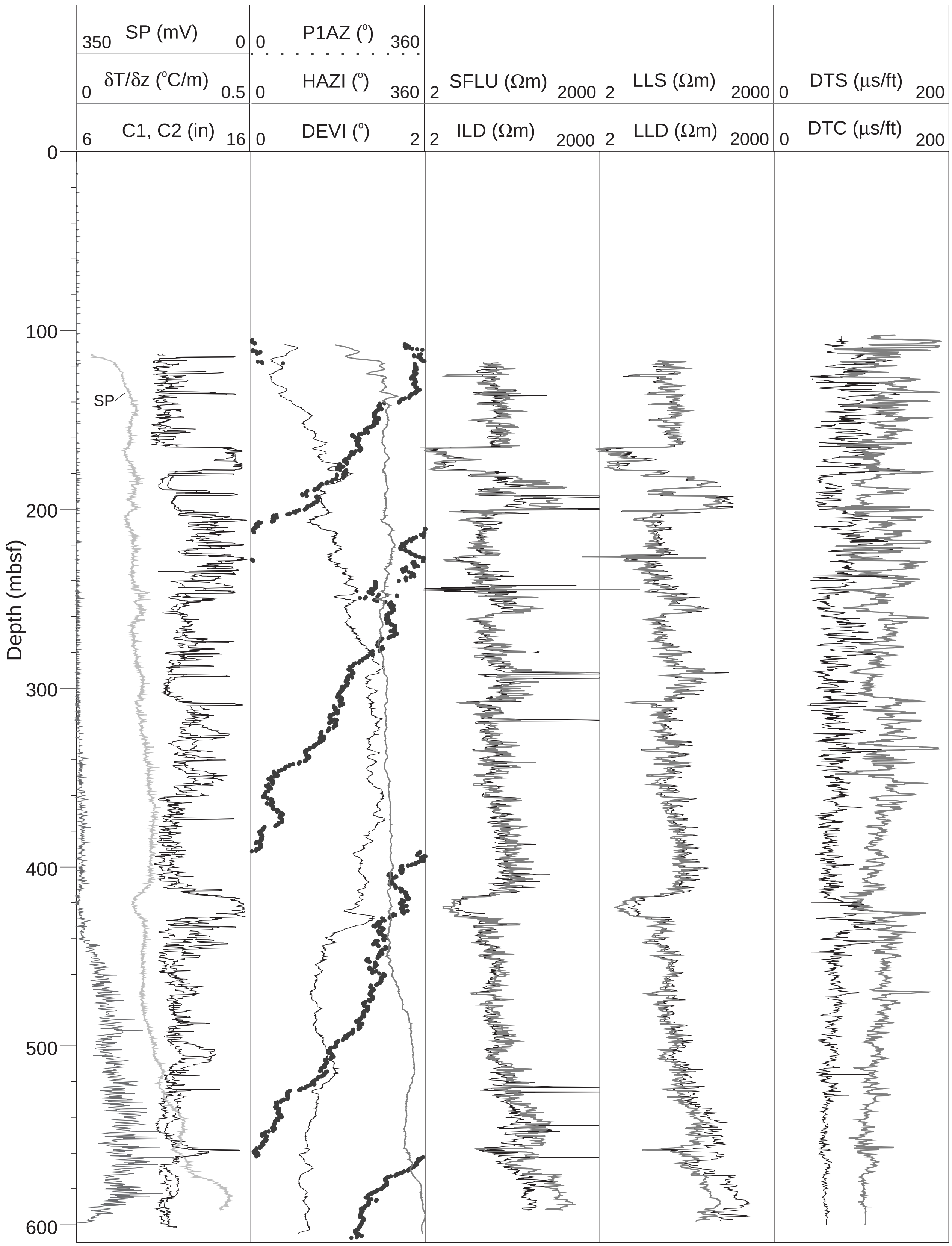

Figure 7. Composite log of hole parameters, electrical logs, and sonic logs recorded during Leg 174B in Hole 395A. Track 1: spontaneous potential (SP), temperature gradient (δT/δz), and calipers C1 and C2 from the FMS tool. Track 2: Pad 1 azimuth of the FMS tool (P1AZ), hole azimuth (HAZI), and hole deviation (DEVI). Track 3: spherical focused log (SFLU) and induction log deep (IDL). Track 4: Laterolog shallow and deep (LLS and LLD). Track 5: traveltimes for the shear (DTS) and compressional (DTC) waves.

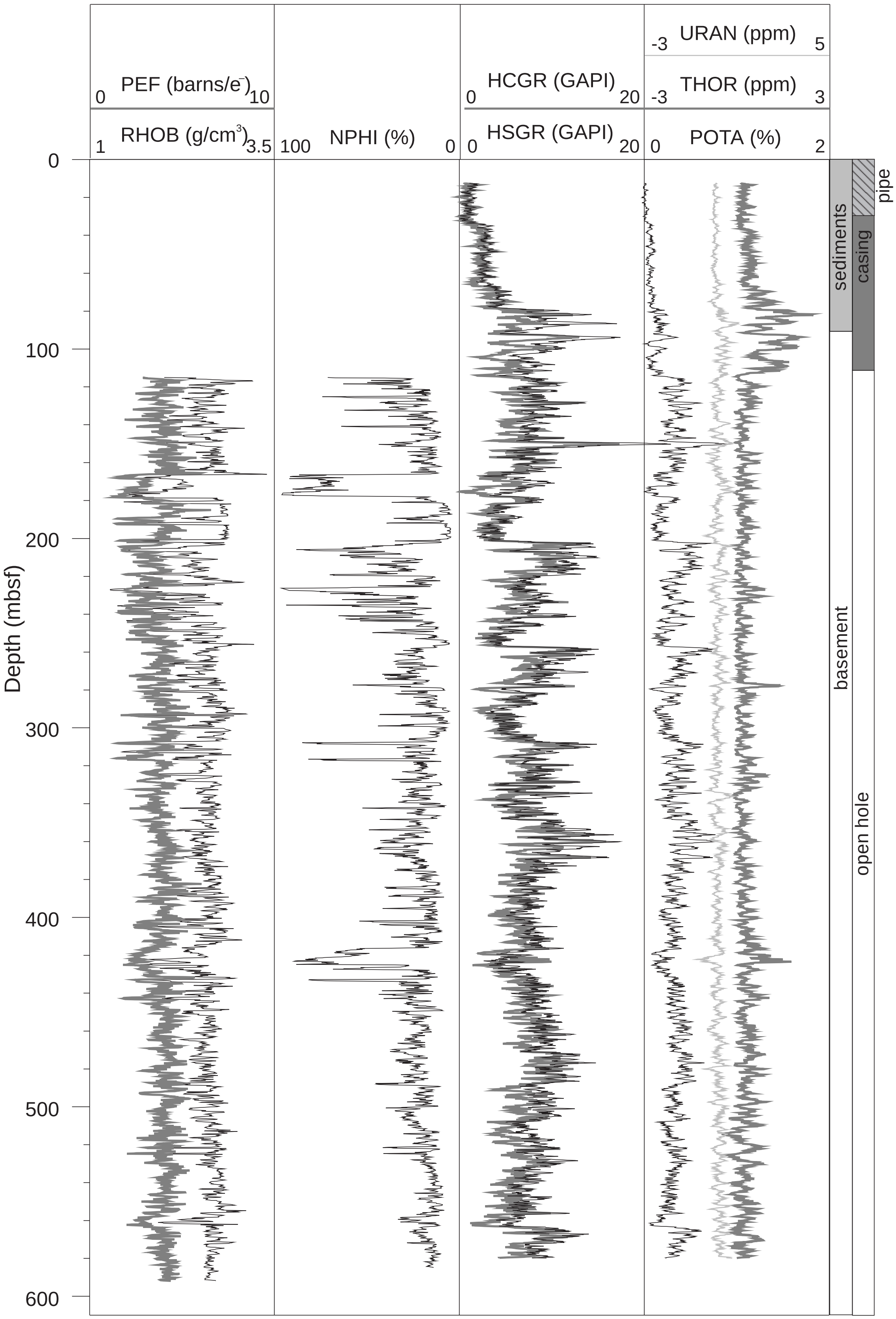

Figure 8. Composite log of the nuclear logs and spectral gamma-ray logs recorded in Hole 395A during Leg 174B. Track 1: photoelectric factor (PEF) and density (RHOB). Track 2: neutron porosity (NPHI). Track 3: computed gamma ray (HCGR) and total spectral gamma ray (HSGR). Track 4: contents of uranium (URAN), thorium (THOR), and potassium (POTA).

conditions of Hole 395A are generally adequate for the acquisition of high-quality data using most logging tools. Hole 395A has also remained relatively circular in cross-section, with few intervals having large systematic differences between the two calipers. The orientation of the calipers with respect to magnetic north (PAZ1 in Track 2) illustrates a relatively constant rate of rotation of the logging tool as it is pulled uphole. This is also indicative of a circular borehole without large breakouts, key slots, or elliptical intervals. Small-scale variations in tool rotation are likely related to localized and minor changes in the shape of the borehole.

Figure 7 (Track 2) also shows the hole deviation and azimuth logs. In general, Hole 395A is nearly vertical, having a slightly increasing deviation below casing to ~1.5° off vertical at 350 mbsf. The hole deviation decreases to 0.75° off vertical at TD. The direction of this deviation rotates from N60°W at the casing shoe to north at the bottom of the hole. This low angle of hole deviation does not affect the operation of the logging tools. With the exception of the two washout intervals noted above, the overall quality of the log data acquired during Leg 174B is excellent.

Temperature Measurements

The temperature gradient log is presented in Figure 7 (Track 1). The raw temperature data recorded with the TLT and the DVTP tools (see "Introduction" chapter, this volume, and the "CORK/DVTP" section, this chapter) agree precisely at coincident station depths. Figure 9 shows a computation from high-resolution TLT data of the continuous temperature gradient profile. This curve illustrates the inversion of the temperature gradient in well-defined intervals in Hole 395A. Two broad inversions occurs between 250 and 300 mbsf and 380 and 420 mbsf, with the large distinct decreases in thin zones between 294 and 298 mbsf and 405 and 420 mbsf. Several smaller drops in the temperature gradient also occur near 200 and 550 mbsf. These zones can be defined with high resolution and indicate that cool seawater is flowing down Hole 395A and exiting the borehole through permeable aquifers in the surrounding formation.

Electrical Resistivity Measurements and Images

Electrical resistivity measurements and images were recorded during each of the three logging runs. An SP log, five different electrical logs (deep laterolog [LLD], shallow laterolog [LLS], spherically focused log [SFL], medium induction resistivity [ILM], and deep induction resistivity [ILD]), and two types of formation images (ARI and FMS) were obtained in Hole 395A during Leg 174B.

The SP curve is presented in Figure 7 (Track 1). In the basaltic upper ocean crust drilled with seawater, SP changes are caused by membrane and streaming potentials (Revil et al., 1997). Whereas the membrane potential is related to the presence of alteration minerals resulting from hydrothermal circulation, the streaming potential is associated with fluid circulation in the hole. The general trend of the SP profile is consequently anticorrelated with that of electrical resistivity, as alteration decreases with resistivity increase, therefore reducing the membrane potential. Local increases in SP over enlarged intervals (see Fig. 7, Track 1), which were identified in the core as rubble sections, are the result of fluid movement from the borehole into the formation. The major section of fluid outflow into basement is located at 420 mbsf, where the temperature gradient changes abruptly from very low values above to larger ones below. Several minor outflow zones are also detected in the SP and temperature gradient profiles at 115, 165, 205, and 560 mbsf.

Five independent measurements of electrical resistivity were recorded with the dual laterolog (DLL; LLD and LLS, as part of the ARI) and the DITE, which also comprises an SFL array. Whereas the galvanic measurements (LLD, LLS, and SFL) are very similar and almost identical to the SFL profile obtained during Leg 109, inductive measurements (ILD and ILM) provide generally lower values, although following closely the same overall profile. This difference is the result of the nature of inductive measurements, where circular current loops are generated in the plane orthogonal to the borehole axis. When used in a vertical hole such as Hole 395A, the induction tool records the horizontal component of the formation resistivity. In a layered formation such as that expected from the core in Hole 395A, inductive measurements are consequently expected to read lower values that galvanic ones.

The lowest values of electrical resistivity are obtained in 12-m-thick rubble sections at 165 and 420 mbsf. The highest values correspond to the presence of thin and massive flows at 180, 195, and 295 mbsf, for example. In sections with resistivity values beyond 200 Ωm, the induction measurements may provide erratic measurements identified with an apparent local increase. This error is of electronic origin, as the secondary magnetic field induced by current loops into the rock is not large enough to be picked by the receiving coils. Such erratic measurements are illustrated in the ILD profile at 190, 290, 315, 525, 545, and 565 mbsf. Another local and erroneous record was obtained with the DLL at 420 mbsf, as the potential reference electrode located 25.5 m above was passing by a massive flow. This phenomenon is related to the Groningen effect and also affects the ARI images.

Two different types of images (ARI and FMS) were recorded in Hole 395A. The shallow reaching, centimeter-scale FMS images both lithologic contacts and millimeter-scale fractures, whereas the deeper penetrating, decimeter-scale ARI is suitably adapted to the identification of lithologic boundaries and aquifers (Figs. 7, 10). The ARI produced images that show the character and orientation of in-

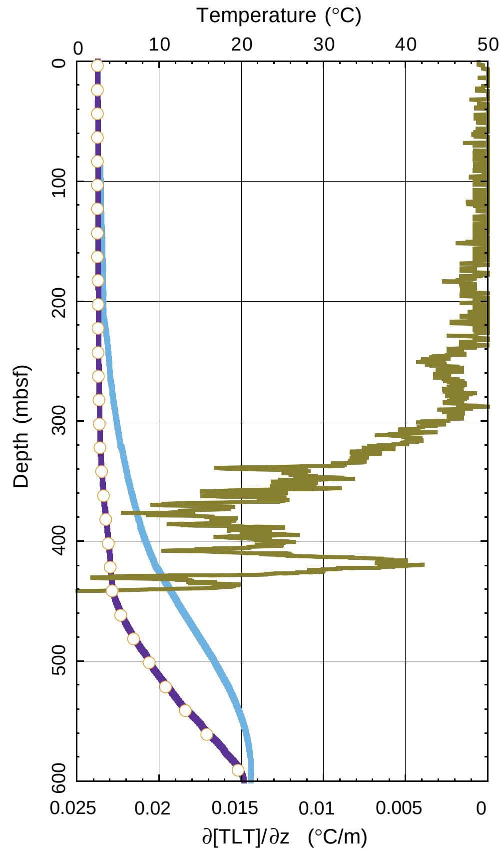

Figure 9. Temperature logs recorded during Leg 174B in Hole 395A. The circles show the station measurements recorded with the Davis-Villinger Temperature Probe (DVTP, °C), the black line corresponds to the downgoing TLT log, and the light gray line corresponds to the upgoing TLT log. The gradient of the downgoing TLT log is shown as dark gray line on the right-hand side in °C/m. The main zone of fluid inflow into the formation is indicated by the sharp temperature gradient decrease at 420 mbsf.

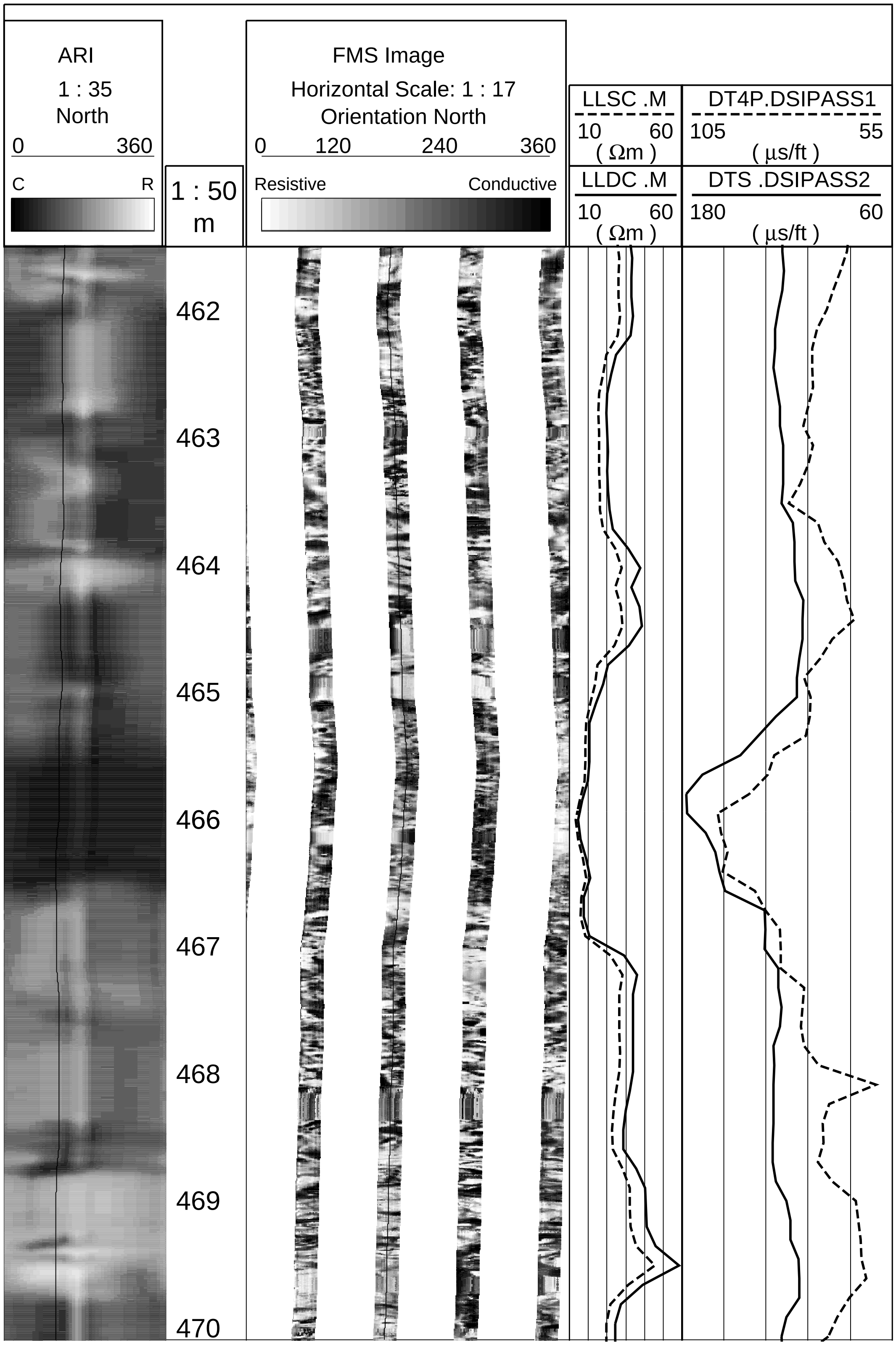

Figure 10. Comparison between ARI recordings, FMS images, resistivity logs (LLSC and LLDC), *P*-wave velocity (DT4P), and shear-wave velocity (DTS) between 462 and 470 mbsf. The 1-m-thick dark interval at 468 mbrf in the ARI image corresponds to a porous zone, and the high-resistivity massive layer near 471 mbsf corresponds to distinct anomalies in the resistivity and sonic logs. The FMS images show considerably greater resolution of the relative conductivity changes over this interval and reflect formation characteristics that are not apparent at the broad scale of the other logs.

dividual pillow basalts and the heterogeneity of crustal structures at a vertical scale of ~1 m. These features are particularly relevant to the hydrogeological structure in Hole 395A and illustrate the physical state of the ocean crust in unprecedented detail. From the comparison of FMS and ARI images, the extent of pillows and flows near the borehole may also be distinguished.

Sonic Measurements

The sonic logs recorded using the DSI tool represent the first use of this tool in the ocean crust. These data were recorded during the second logging run with three separate passes of the tool through the open-hole interval. In total, five different modes of the DSI were enabled (see "Introduction" chapter, this volume) and allowed for acquisition of both compressional and shear waveforms using different acoustic sources. Both high-frequency compressional and shear and dipole shear modes produced excellent quality sonic waveforms. Preliminary data processing for compressional (DTC) and shear (DTS) travel times was completed on the drill ship using Slowness-Time-Coherence (STC) analysis software on the Schlumberger MAXIS acquisition system (Kimball and Marzetta, 1984). Postcruise processing must also be applied to the dipole data to account for dispersion effects, which may reduce the travel times by 2%–6% (Brie and Saiki, 1996). The low-frequency Stoneley mode produced unreliable waveforms and is not discussed further.

The DTC and DTS logs through the open hole are shown in Figure 7, Track 5. DTC was computed using the high-frequency source over a range from 30 to 150 µs/ft; DTS was computed from the low-frequency dipole source over a range from 70 to 200 µs/ft. The compressional wavelength is ~30 cm in these formations, whereas the shear wavelength is ~1 m. The quality of these computations is directly related to the waveform coherence between receivers (not shown), which is high overall and generally greater than 50% for the dipole-shear data. Both compressional and shear-wave coherence is degraded in washouts and with frequent excursions in hole size, which tends to reduce data quality above 240 mbsf and near 420 mbsf. The dipole-shear waveforms also have systematically higher coherence than the high-frequency compressional and high-frequency shear waveforms, which is in part the result of less scattering from small fractures and pillow basalt morphologies affecting the shorter wavelengths.

The compressional and shear travel time logs show an increasing trend with depth, anticorrelated with the electrical resistivity and density logs. The average value of compressional and shear travel times generally agree with the multichannel sonic log results from Leg 109 (Moos, 1990) with V_p/V_s ratios averaging ~1.7 in massive units and ranging between 1.8 and 2.2 in pillow basalts. Fine-scale variations in the compressional and shear travel times illustrate the lithologic and hydrogeologic character of Hole 395A. In Figure 10, an interval from 462 to 470 mbsf is displayed using the GeoFrame software package to compare deep and shallow penetrating resistivity images (ARI and FMS in Tracks 1 and 2, respectively) with deep and shallow resistivity logs (LLD and LLS in Track 3) and compressional and shear travel time logs (DTC and DTS in Track 4). Both the high-conductivity porous zone near 466 mbsf and the high-resistivity massive layer near 469 mbsf correlate to anomalies in all of the logs. The FMS images show considerably greater resolution of the relative conductivity changes over the interval and reflect formation characteristics that are not apparent at the broad scale of the other logs.

Nuclear Measurements

The bulk density (RHOB) of the formation and the photoelectric factor (PEF) were measured using the LDS tool and are displayed in Figure 8 (Track 1). Density values range from 1.3 to >3.0 g/cm^3, and the log shows rapid variations as a function of depth. Low-density values are related to fractures filled with seawater or to enlarged sections of the hole. Typical values of ~2.95 g/cm^3 for basalt are recorded over intervals with good borehole conditions. The PEF varies between 1 and 5 barns/e$^-$, which are also typical values for basalt.

The APS tool was used to record the neutron porosity log (NPHI) and is shown in Figure 8 (Track 2). NPHI ranges from 5% to 100%. High values correspond with borehole washouts or fractures and generally correlate with low peaks in the density log. NPHI also decreases slightly with depth, which may be attributed to a decrease in fracturing observed in the FMS images.

The spectral gamma-ray logs in Figure 8 (Tracks 3 and 4) were measured using the HNGS tool (Shipboard Scientific Party, in press). The total spectral gamma ray (HSGR) varies between 2 and 20 GAPI in Hole 395A. The HSGR, the computed gamma ray (HCGR), and the potassium content (POTA) also show a strong correlation in the pillow basalts and flows, indicating that most of the natural radioactivity is caused by the potassium rather than the thorium (THOR) or uranium (URAN) decay series. Potassium is enriched in oceanic basalts during low temperature oxidative alteration, and thus, HSGR and POTA logs are good indicators of alteration. Within the cased interval of Hole 395A (seafloor to 113 mbsf), HSGR and HCGR logs decrease gradually upwards and correlate with THOR. These through-casing logs indicate that thorium is the most important radioactive element in the sediments near Hole 395A.

Lithostratigraphy

Based on log and core analysis at this site during previous legs, it is well known that Hole 395A consists of pillow basalts and massive basalt flows. These formations can be distinguished using the electrical resistivity, density, neutron porosity, and spectral gamma-ray logs. For example, two massive lava flows observed in the cores can be identified in the log responses between 178 and 202 mbsf and 242 and 259 mbsf. They are characterized by an increase in the LLD resistivity by up to 400 Ωm. NPHI is generally low and typically remains <10%. The density values are high, and RHOB generally ranges between 2.7 and 2.9 g/cm^3. HSGR values are <6 GAPI in the massive flows, and POTA is <0.3%. Most of the logs also show sharp peaks that indicate fracturing or thin intercalation of pillow basalt within the massive flows. Because of the low core recovery (~18%) in Hole 395A, it is important to note that the thickness of the massive flows derived from the logs is generally less than that estimated from the cores (Shipboard Scientific Party, 1979). However, massive flows generally have higher recovery than pillow basalts, and their thicknesses are often overestimated from core analyses.

The pillow basalts in Hole 395A correspond with a broad range of values in the logs. This variability in log response is caused by variations in hole size, which affects most logs, and by the varying intensity of alteration and fracturing in pillow basalt. Typical log responses in pillows have LLD <100 Ωm, NPHI exceeding 20%, and HSGR values between 5 and 20 GAPI. An apparent cyclicity in the logs is observed in the pillows, and is most distinct in the HSGR, POTA, and the resistivity logs. These cycles were also observed in the log data from Legs 78B and 109 (Hyndman and Salisbury, 1984; Moos, 1990). They show HSGR and POTA increasing upwards from low to high values in each cycle and are likely related to the concentration of alteration minerals within different units. Distinct boundaries between these units can be observed at 202, 259, 307, 348, 407, and 563 mbsf.

REFERENCES

Anderson, R.N., and Zoback, M.D., 1982. Permeability, underpressures, and convection in the oceanic crust near the Costa Rica Rift, eastern equatorial Pacific. *J. Geophys. Res.,* 87:2860–2868.

Becker, K., 1990. Measurements of the permeability of the upper oceanic crust at Hole 395A, ODP Leg 109. *In* Detrick, R., Honnorez, J., Bryan, W.B., Juteau, T., et al., *Proc. ODP, Sci. Results,* 106/109: College Station, TX (Ocean Drilling Program), 213–222.

Becker, K., and Davis, E.E., 1998. CORK reveals huge fluxes in off-axis hydrologic circulation. *JOI/USSAC Newsletter,* 11:12–15.

Becker, K., Langseth, M.G., and Hyndman, R.D., 1984. Temperature measurements in Hole 395A, Leg 78B. *In* Hyndman, R.D., Salisbury, M.H., et al., *Init. Repts. DSDP,* 78B: Washington (U.S. Govt. Printing Office), 689–698.

Becker, K., Langseth, M.G., and Von Herzen, R.P., 1983a. Deep crustal geothermal measurements, Hole 504B, Deep Sea Drilling Project Legs 69 and 70. *In* Cann, J.R., Langseth, M.G., Honnorez, J., Von Herzen, R.P., White, S.M., et al., *Init. Repts. DSDP,* 69: Washington (U.S. Govt. Printing Office), 223–236.

Becker, K., Langseth, M.G., Von Herzen, R.P., and Anderson, R.N., 1983b. Deep crustal geothermal measurements, Hole 504B, Costa Rica Rift. *J. Geophys. Res.,* 88:3447–3457.

Becker, K., Langseth, M.G., Von Herzen, R.P., Anderson, R.N., and Hobart, M.A., 1985. Deep crustal geothermal measurements, Hole 504B, Deep Sea Drilling Project Legs 69, 70, 83, and 92. *In* Anderson, R.N., Honnorez, J., Becker, K., et al., *Init. Repts. DSDP,* 83: Washington (U.S. Govt. Printing Office), 405–418.

Becker, K., the Leg 174B Scientific Party, and Davis, E.E., 1998. Leg 174B revisits Hole 395A: logging and long-term monitoring of off-axis hydrothermal processes in young oceanic crust. *JOIDES J.,* 24:1–3, 13.

Becker, K., Morin, R.H., and Davis, E.E., 1994. Permeabilities in the Middle Valley hydrothermal system measured with packer and flowmeter experiments. *In* Mottl, M.J., Davis, E.E., Fisher, A.T., and Slack, J.F. (Eds.), *Proc. ODP, Sci. Results,* 139: College Station, TX (Ocean Drilling Program), 613–626.

Becker, K., Sakai, H., Adamson, A.C., Alexandrovich, J., Alt, J.C., Anderson, R.N., Bideau, D., Gable, R., Herzig, P.M., Houghton, S.D., Ishizuka, H., Kawahata, H., Kinoshita, H., Langseth, M.G., Lovell, M.A., Malpas, J., Masuda, H., Merrill, R.B., Morin, R.H., Mottl, M.J., Pariso, J.E., Pezard, P.A., Phillips, J.D., Sparks, J.W., and Uhlig, S., 1989. Drilling deep into young oceanic crust, Hole 504B, Costa Rica Rift. *Rev. Geophys.,* 27:79–102.

Brie, A., and Saiki, Y., 1996. Practical dipole sonic dispersion correction. *Trans. Soc. Expl. Geophys*., 6:178–181.

Bryan, W.B., Juteau, T., et al., 1988. *Proc. ODP, Init. Repts.,* 109: College Station, TX (Ocean Drilling Program).

Davis, E.E., Becker, K., Pettigrew, T., Carson, B., and MacDonald, R., 1992. CORK: a hydrologic seal and downhole observatory for deep-ocean boreholes. *In* Davis, E.E., Mottl, M.J., Fisher, A.T., et al., *Proc. ODP, Init. Repts.,* 139: College Station, TX (Ocean Drilling Program), 43–53.

Davis, E.E., Mottl, M.J., Fisher, A.T., et al., 1992. *Proc. ODP, Init. Repts.,* 139: College Station, TX (Ocean Drilling Program).

Erickson, A.J., Von Herzen, R.P., Sclater, J.P., Girdler, R.W., Marshall, B.V., and Hyndman, R.D., 1975. Geothermal measurements in deep-sea boreholes. *J. Geophys. Res.,* 80:2515–2528.

Gable, R., Morin, R.H., and Becker, K., 1989. Geothermal state of Hole 504B: ODP Leg 111 overview. *In* Becker, K., Sakai, H., et al., *Proc. ODP, Sci. Results,* 111: College Station, TX (Ocean Drilling Program), 87–96.

————, 1992. Geothermal state of DSDP Holes 333A, 395A and 534A: results from the DIANAUT program. *Geophys. Res. Lett.,* 19:505–508.

Guerin, G., Becker, K., Gable, R., and Pezard, P.A., 1996. Temperature measurements and heat-flow analysis in Hole 504B. *In* Alt, J.C., Kinoshita, H., Stokking, L.B., and Michael, P.J. (Eds.), *Proc. ODP, Sci. Results,* 148: College Station, TX (Ocean Drilling Program), 291–296.

Hickman, S.H., Langseth, M.G., and Svitek, J.F., 1984. *In situ* permeability and pore-pressure measurements near the Mid-Atlantic Ridge, Deep Sea Drilling Project Hole 395A. *In* Hyndman, R.D., Salisbury, M.H., et al., *Init. Repts. DSDP,* 78B: Washington (U.S. Govt. Printing Office), 699–708.

Hussong, D.M., Fryer, P.B., Tuthill, J.D., and Wipperman, L.K., 1979. The geological and geophysical setting near DSDP Site 395, north Atlantic Ocean. *In* Melson, W.G., Rabinowitz, P.D., et al., *Init. Repts. DSDP,* 45: Washington (U.S. Govt. Printing Office), 23–37.

Hyndman, R.D., Salisbury, M.H., et al., 1984. *Init. Repts. DSDP,* 78B: Washington (U.S. Govt. Printing Office).

Hyndman, R.D., and Salisbury, M.H., 1984. The physical nature of young upper oceanic crust on the Mid-Atlantic ridge, Deep Sea Drilling Project Hole 395A. *In* Hyndman, R.D., Salisbury, M.H. et al., *Init. Repts. DSDP*, 78B: Washington (U.S. Govt. Printing Office), 839–848

Hyndman, R.D., Von Herzen, R.P., Erickson, A.J., and Jolivet, J., 1976. Heat flow measurements in deep crustal holes on the Mid-Atlantic Ridge. *J. Geophys. Res.*, 81:4053–4060.

Kimball, C.V., and Marzetta, T.L., 1984. Semblance processing of borehole acoustic array data. *Geophysics,* 49:274–281.

Kopietz, J., Becker, K., and Hamano, Y., 1990. Temperature measurements at Site 395, ODP Leg 109. *In* Detrick, R., Honnorez, J., Bryan, W.B., Juteau, T., et al., *Proc. ODP, Sci. Results,* 106/109: College Station, TX (Ocean Drilling Program), 197–203.

Langseth, M.G., Becker, K., Von Herzen, R.P., and Schultheiss, P., 1992. Heat and fluid flux through the sediment on the western flank of the Mid-Atlantic Ridge: a hydrological study of North Pond. *Geophys. Res. Lett.,* 19:517–520.

Langseth, M.G., Hyndman, R., Becker, K., Hickman, S.H., and Salisbury, M., 1984. The hydrogeolological regime of isolated sediment ponds in mid-oceanic ridges. *In* Hyndman, R.D., Salisbury, M.H., et al., *Init. Repts. DSDP,* 78 (Pt. 2): Washington (U.S. Govt. Printing Office), 825–837.

Moos, D., 1990. Petrophysical results from logging in DSDP Hole 395A, ODP Leg 109. *In* Detrick, R., Honnorez, J., Bryan, W.B., Juteau, T., et al., *Proc. ODP, Sci. Results,* 106/109: College Station, TX (Ocean Drilling Program), 237–253.

Morin, R.H., Hess, A.E., and Becker, K., 1992. In situ measurements of fluid flow in DSDP Holes 395A and 534A: results from the DIANAUT program. *Geophys. Res. Lett.,* 19:509–512.

Revil, A., Pezard, P.A., and Darot, M., 1997. Electrical conductivity, spontaneous potential and ionic diffusion in porous media. *In* Lovell, M.A., and Harvey, P.K. (Eds.), *Developments in Petrophysics,* Geol. Soc. Spec. Publ. London, 122:253–275.

Shipboard Scientific Party, in press. Explanatory notes. *In* Keigwin, L., and Rio, D., *Proc. ODP, Init. Repts.,* 172: College Station, TX (Ocean Drilling Program).

————, 1979. Site 395: 23°N, Mid-Atlantic Ridge. *In* Melson, W.G., Rabinowitz, P.D., et al., *Init. Repts. DSDP,* 45: Washington (U.S. Govt. Printing Office), 131–264.

————, 1988. Site 395. *In* Bryan, W.B., Juteau, T., et al., *Proc. ODP Init. Repts.*, 109: College Station, TX (Ocean Drilling Program), 175–202.

Ms 174BIR-102

NOTE: Shore-based log processing data can be found on CD-ROM (back pocket of this volume). See Table of Contents for material contained on CD-ROM.